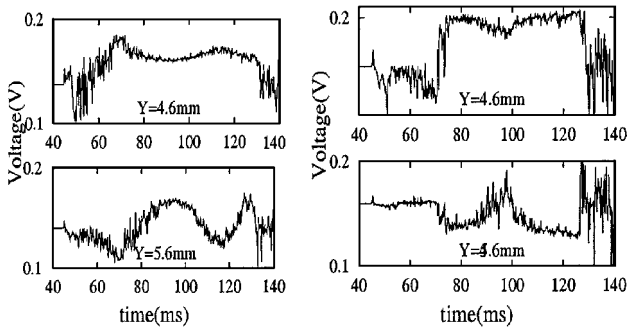

a) $X/L = 0.80$ b) $X/L = 0.86$

Fig. 7 Simultaneous time traces of voltage signals near the main shock region (above the bubble); P_0 = 50 bar.

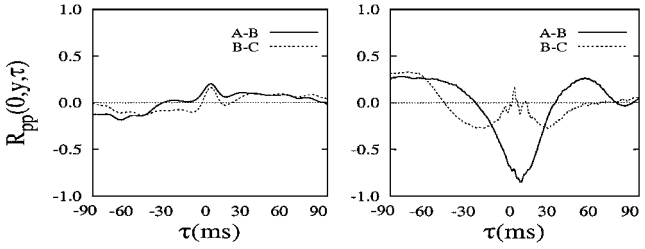

a) $X/L = 0.40$ b) $X/L = 0.66$

Fig. 8 Space-time correlation functions for photodiode locations (close to the surface) near the oscillating separation shock; P_0 = 50 bar.

Figure 8 shows the space-time correlation $R_{pp}(0, y, \tau)$ for channels separated in the Y direction, as a function of time delay τ (milliseconds) between the voltage signals from A and B and locations B and C. The point of interest is the value of the correlation at approximately zero time delay. Far upstream of separation (Fig. 8a) the plot shows a positive value for locations A–B and B–C. For axial locations $X/L = 0.40, 0.66$, A is $Y = 0.6$ mm from the surface, whereas B and C are $Y = 1.6$ and 2.6 mm, respectively, away from the surface. For downstream locations A is $Y = 1.6$ mm from surface, whereas B and C are $Y = 2.6$ and 3.6 mm, respectively, away from model surface. These distances were chosen wherever mirror imaging of signals from neighboring channels were observed and indicates that all locations experience similar density flow with the absence of any fluctuating density gradients. At separation (Fig. 8b) the space-time correlation value between these locations show opposite trends. Locations A and B (which are in close proximity to one another) show a large negative value, whereas B and C show a relatively large positive value indicating that, when photodiode A experiences a rise in density (as across a shock), the photodiode B experiences a fall and vice versa. Locations B and C experience a similar rise and fall of density.

Conclusions

The unsteadiness associated with the shock-wave boundary-layer interaction (SWBLI) flowfield on a HALIS axisymmetric configuration model is demonstrated in a Mach 9.68 flow with air as test gas. The SWBLI flowfield investigated generates high-pressure loads in the vicinity of separation and reattachment points. Near reattachment the pressure on the flare approaches the stagnation point pressure level. Off-surface flow study using the laser schlieren system revealed increased energy levels near the separation point suggesting random fluctuations in the instantaneous position of the separation shock. Space-time correlation of voltage signals from neighboring channels, exhibiting mirror-imaging effects, shows a negative value at zero time delay. The observation is consistent with the view that the separation shock translates back and forth, in response to the expansion and contraction motion of the separation bubble, in the vicinity of separation point on the HAC model, and hence is responsible for high-pressure loads at these locations.

References

[1]Kistler, A. L., "Fluctuating Wall Pressure Under a Separated Supersonic Flow," *Journal of the Acoustical Society of America*, Vol. 36, No. 3, 1964, pp. 543–550.

[2]Dolling, D. S., and Murphy, M. T., "Unsteadiness of the Separation Shock Wave Structure in a Supersonic Compression Ramp Field," *AIAA Journal*, Vol. 21, No. 12, 1983, pp. 1628–1634.

[3]Maull, D. J., "Hypersonic Flow over Axially Symmetric Spiked Bodies," *Journal of Fluid Mechanics*, Vol. 8, Pt. 4, 1969, pp. 584–592.

[4]Dolling, D. S., and Bogdonoff, S. M., "An Experimental Investigation of the Unsteady Behaviour of Blunt Fin-Induced Shock Wave Turbulent Boundary layer Interaction," AIAA Paper 81-1287, June 1981.

[5]Horstman, C. C., and Owen, F. K., "New Diagnostic Technique for the Study of Turbulent Boundary Layer Separation," *AIAA Journal*, Vol. 12, No. 10, 1974, pp. 1436–1438.

[6]Verma, S. B., and Koppenwallner, G., "Experimental Study of Shock Unsteadiness on an Hyperboloid Model Using Laser Schlieren," *9th AG-STAB Workshop*, edited by H. J. Heinemann, DLR-Standort, Göttingen, Germany, 1999, pp. 156, 157.

[7]Koppenwallner, G., Friehmelt, H., and Muller-Eigner, R., "Calibration and First Results of Redesigned Ludwieg Expansion Tube," AIAA Paper 93-5001, Nov. 1993.

[8]Funk, B. H., and Johnston, K. D., "Laser Schlieren Cross-Beam Measurements in a Supersonic Jet Shear Layer," *AIAA Journal*, Vol. 8, No. 11, 1970, pp. 2074, 2075.

[9]Garg, S., and Settles, G. S., "Unsteady Pressure Loads Generated by Swept-Shock-Wave/Boundary-Layer Interactions," *AIAA Journal*, Vol. 34, No. 6, 1996, pp. 1174–1181.

[10]Willmarth, W. W., Kuethe, A. M., and Crocker, G. H., "Stagnation Point Fluctuations on a Body of Revolution," *Physics of Fluids*, Vol. 2, No. 6, 1959, pp. 714–716.

M. Torres
Associate Editor

Modeling of Performance of an Artillery Shell Using Neural Networks

A. K. Ghosh,* S. C. Raisinghani,† and S. K. Dehury‡
Indian Institute of Technology Kanpur, Kanpur 208016, UP, India

Introduction

ARTILLERY comprises an important wing of an army in providing firepower, during both war and cross-border skirmishes with the enemy. Artillery shells are a class of projectiles around which much of aeroballistic theory was originally developed, and it continues to form a significant part of aeroballistician's interest. The performance of the artillery shell is governed by many factors, such as muzzle velocity irregularity, jump and throw off; ambient meteorological conditions such as temperature, density, head/tailwind, and crosswind; and manufacturing procedures resulting in differences in shape, size, mass, and yawing behavior. The conventional approach hitherto used for predicting behavior and performance of a projectile such as an artillery shell was via mathematical models.[1]

Beginning with the simplest, but relatively inaccurate, in-vacuo trajectory mathematical model, more and more sophisticated models of increasing accuracy, such as the point mass model, the modified point mass model, and the six-degree-of-freedom model, have been developed. However, even the best of these models have their limitations because of 1) an inability to model all of the problem variables (e.g., the initial conditions at the time of shell leaving the barrel, the jump and throw off, the variable atmospheric conditions,

Received 1 May 2001; revision received 10 February 2002; accepted for publication 18 February 2002.

*Assistant Professor, Department of Aerospace Engineering. Member AIAA.

†Professor, Department of Aerospace Engineering. Senior Member AIAA.

‡Graduate Student, Department of Aerospace Engineering.

etc.) and 2) the nonavailability of accurate and reliable aerodynamic coefficients (e.g., drag coefficient, damping-in-roll derivative, etc.) required as inputs by the mathematical models.

The recent interest in the evolving applications of artificial neural networks (ANNs) to diverse fields such as signal processing, pattern recognition, robotics, medical diagnosis, system identification, and control have led many researchers to explore their capability for aerospace engineering problems. The neural modeling has been employed in solving aerospace problems such as aerodynamic modeling,[2] buffet,[3] fatigue crack growth,[4] design of a civil aircraft,[5] aircraft parameter estimation from flight data,[6,7] etc. In the present work, an attempt is made to develop a neural model for predicting the performance of an artillery shell under known ambient atmospheric conditions. Because the field data on the performance of artillery shells have a number of noisy parameters that interact in a nonlinear manner, the neural modeling is an attractive alternative to the traditional mathematical modeling and regression techniques. The neural modeling has the ability to accommodate nonlinearties and to generalize from the data shown during the training sessions. The latter property is especially useful when one has to model sparse real data from field trials of artillery shells.

Artillery Shell Data and Modeling

The performance data for artillery shells are generally available in the form of range tables. Typically, range table might list the range R obtainable for various firing (elevation) angles θ under standard calm atmospheric conditions for a shell having nominal mass m and fired with a nominal muzzle velocity V. Also listed are the time of flight T and the lateral drift in terms of correction to bearing angle Ψ that would be required to hit the target. Information is provided for correcting R, T, and Ψ for 1) variations in the ambient atmospheric conditions (air temperature t and density ρ being different from those corresponding to standard atmosphere), 2) the presence of a head/tailwind W_x and crosswind W_z, and 3) the mass of the shell and muzzle velocity, being different from the corresponding nominal values. Generally, range tables are prepared based on a chosen mathematical model that is adjusted and validated for a few measured data. This may require introduction of a few fudge factors to achieve reasonable matching; a fudge factor used to modify the aerodynamic coefficients might be a constant or a function of problem variables, for example, θ. Although t, ρ, W_x, and W_z vary along the path of the projectile, the corrections provided for these in the range tables are based on some equivalent constant (average) values. Note that it is possible to account for the varying wind and atmospheric conditions in some of the proposed mathematical models.[8] However, the inverse problem of finding the firing angle for a specified range and existing ambient conditions can not be directly solved via mathematical models, and one has to rely on the range table for an answer. It is in this context that the proposed neural approach is shown to yield an answer as easily to the inverse problem as it does to the direct problem.

The performance data for an artillery shell (B-shell) were supplied by Armament Research and Development Establishment, Pune, India. The data supplied in the form of range tables have 323 data points, listing R, T, and Ψ as a function of θ under standard atmospheric conditions ($t = 288.0$ K and $\rho = 1.225$ kg/m^3) and calm conditions ($W_x = W_z = 0$) for a shell of nominal mass (42.6 kg) and muzzle velocity (818 m/s). A procedure is also provided to correct the R, T, and Ψ for t, ρ, m, and V being different from the standard (nominal) values and for equivalent head/tail/crosswind. By the use of the basic 323 data points, and applying corrections for an arbitrarily chosen set of atmospheric conditions, mass, and muzzle velocity of shell, as many additional data points can be generated as desired. The data set so generated is used to select appropriate input/output (I/O) pairs for the neural model.

Neural Model

From the point of view of field applications, a soldier would want to know the required firing angle and bearing correction to achieve the required range. The information available before firing in terms of R, t, ρ, W_x, W_z, V, and M is used to form the input vector, whereas the required information in terms of θ, Ψ, and T forms the output variables of the neural model. In the network input file, any deviations from the standard temperature, density, and muzzle velocity are given as percent change from the nominal values, whereas the deviation from the nominal mass is given as the difference between the actual mass and the nominal mass. This scheme was followed after a brief study revealed that such a definition of network input variables yielded better training compared to the use of absolute values of the corresponding variables. The neural model does not require either the postulation of a mathematical/numerical model, nor an estimate of initial conditions at the time of shell leaving the barrel. Whereas functional mapping of the I/O pairs creates a black box type of neural model, the initial conditions are also taken care of implicitly by the mapping. Measured data can be directly used to train the network. However, due to the nonavailability of measured data, the data from the range table are taken as the measured data for the purpose of training, validation, and prediction via the proposed neural model. The feedforward neural networks for the present study were simulated by using the neural network toolbox of MATLAB® 5.3. The activation function used is the sigmoidal function, and a backpropagation algorithm is used for training the network.

A random selection of I/O pairs showed poor training of the network. A close look at the data and consideration the physics of the projectile motion revealed why: As is well known for an idealized point mass projectile motion in vacuum, the range of a projectile increases as θ increases from 0 to 45 deg and then decreases as θ increases beyond 45 deg. A similar trend exists for B-shell also wherein maximum range is obtained at around 45 deg (at 802 mil, 360 deg = 6400 mil). Thus, the neural network sees an inherent contradiction in data that have range and firing angle as I/O pairs spanning the whole range of firing angles, hence the difficulty in mapping such data.

To resolve this difficulty, the data are partitioned into two bins: one set having firing angles below 45 deg and the other above it (up to 70 deg as given in the range table). The neural models for these two ranges of firing angles are separately developed. Note that such an approach will not impose any limitations in practical applications because the requirement that the desirable θ be less than or more than 45 deg would be generally known. If the shell is to achieve high altitude during its flight to target, θ of greater than 45 deg would be recommended, otherwise less than 45 deg would be preferred for its shorter time of flight.

For modeling, a set of I/O pairs selected randomly from each of the bins is used separately for training sessions. Sets of varying number of I/O pairs were used to arrive at a minimum number of I/O pairs required for adequate training of the network. It is acknowledged that in real life, the number of measured I/O pairs available might be limited due to the cost involved in collecting such range data, hence the search for the minimum number of data samples to achieve an acceptable neural model. The numbers of I/O pairs used were varied, to have 100, 50, 25, and 15 samples. Obviously, the higher the number of samples, the better the training, but even as few as 15 samples gave satisfactory levels of training. The suitability of the models is tested by a validation (test) data set, typically consisting of 15 or 30 I/O pairs from the same bin, but other than those used for training. The rule of thumb used is that if, for the validation data, the mean square error (MSE) is only of the order of two times or less than the MSE prescribed for the training phase, the neural model is acceptable, and its architecture is fixed for the next step of prediction phase. If not, the tuning parameters of the network, such as the learning rate, the number of neurons in the hidden layer, the momentum rate, the number of iteration, etc., are varied until the network meets the given conditions for MSE for the training as well as for the validation phase.

For prediction, a set of randomly selected input data is taken from the range table and presented to the validated network. The predicted output is compared with the corresponding values from the range table. Typically, for prediction, 10 samples were randomly selected from the range table. Because the neural model is required to predict more than one output, that is, θ, Ψ, and T, the following study was undertaken to answer the following question: For the same set of inputs, is it better to train the network separately for one output at a time, or to train it on all of the outputs at once? The former approach

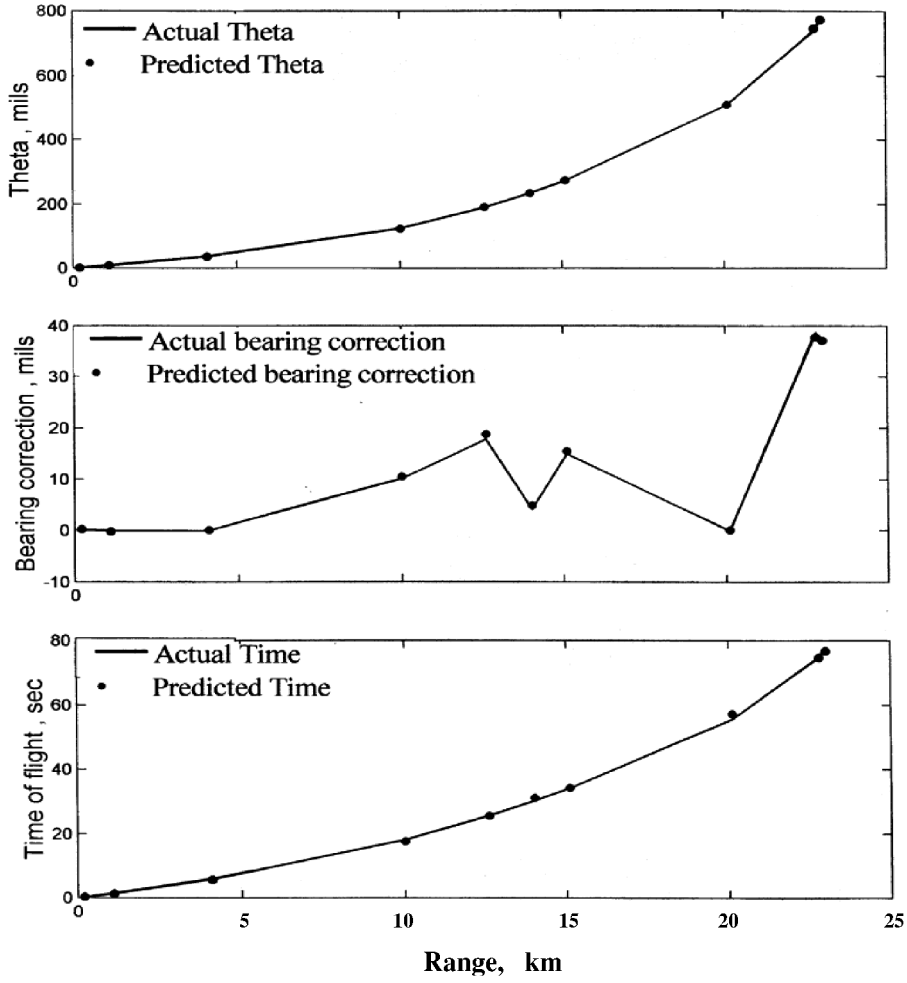

Fig. 1 Comparison of actual and predicted theta, bearing correction, and time of flight.

always yielded relatively more accurate predictions and, therefore, all of the results presented herein are based on the single output option.

Figure 1 shows that the predicted θ, Ψ, and T compare well with those from the range table. Although not discernible from Fig. 1, a close look at the numerical values of predicted and actual θ showed that relatively accurate θ is predicted for the smaller values of θ. The trend was observed repeatedly for many sets of input variables selected for the study. This observed trend could be explained as follows: At the lower end of θ values, the range obtainable is more sensitive to variations in θ. Typically, increase of 1 mil in θ results in range increasing by 134 m for a nominal value of $\theta = 0.7$ mil, but at nominal value of $\theta = 802.3$ mil, a 1-mil increase in θ results in range increasing by only 3.2 m. Notwithstanding this observation, the predicted values by neural model are satisfactory for the whole range of θ.

Conclusions

This study presents an alternative approach to mathematical modeling used hitherto for predicting shell performance in terms of the firing angle needed for the required range. The neural model is shown to be a viable way of modeling many input variables that affect the relationship between the range and the firing angle. It is envisaged that the measured data for shells could be used for developing neural models that would be useful in field applications, including finding the firing angle, the time of flight (this might be required for fuse setting), and the drift angle for the specified range.

Acknowledgment

This research was funded by Armament Research Board (ARMREB), Ministry of Defense, New Delhi. The authors acknowledge the help provided by ARMREB in supplying and interpreting the data of the range tables.

References

[1]"External Ballistics," *Text-Book of Ballistics and Gunnery*, Vol. 1, 1st ed., Her Majesty's Stationary Office, London, 1987, pp. 443–497.

[2]Hess, R. A., "Use of Backpropagation with Feedforward Neural Networks for the Aerodynamic Estimation Problem," AIAA Paper 93-3638, Aug. 1993.

[3]Jacobs, J. H., Hedgecock, C. E., Lichtenwalner, P. F., Pado, L. E., and Washburn, A. E., "Use of Artificial Neural Networks for Buffet Environments," *Journal of Aircraft*, Vol. 31, No. 4, 1994, pp. 831–836.

[4]Pidaparti, R. M. V., and Palakal, M. J., "Neural Network Approach to Fatigue-Crack-Growth Predictions Under Aircraft Spectrum Loadings," *Journal of Aircraft*, Vol. 32, No. 4, 1995, pp. 825–831.

[5]Patnaik, S. N., Guptill, J. D., Hopkins, D. A., and Lavelle, T. M., "Neural Network and Regression Approximations in High-Speed Civil Aircraft Design Optimization," *Journal of Aircraft*, Vol. 35, No. 6, 1998, pp. 839–850.

[6]Ghosh, A. K., Raisinghani, S. C., and Khubchandani, S., "Estimation of Aircraft Lateral-Directional Parameters Using Neural Networks," *Journal of Aircraft*, Vol. 35, No. 6, 1998, pp. 876–881.

[7]Ghosh, A. K., and Raisinghani, S. C., "Frequency-Domain Estimation of Parameters from Flight Data Using Neural Networks," *Journal of Guidance, Control, and Dynamics*, Vol. 24, No. 3, 2001, pp. 525–530.

[8]James, R. L., Jr., "A Three-Dimensional Trajectory Simulation Using Six Degrees of Freedom with Arbitrary Wind," NASA TN D-641, 1961.

M. S. Miller
Associate Editor